Microwave-excited Microplasma Thruster with Applied Magnetic Field

IEPC-2011-262

Presented at the 32nd International Electric Propulsion Conference,
Wiesbaden • Germany
September 11 – 15, 2011

Tetsuo Kawanabe[1], Takeshi Takahashi[2], Yoshinori Takao[3], Koji Eriguchi[4] and Kouichi Ono[5].
Department of Aeronautics and Astronautics, Graduate School of Engineering,
Kyoto University, Yoshida-Honmachi, Sakyo-ku, Kyoto 606-8501, Japan

Abstract: This paper describes the thrust performance of an electrothermal microplasma thruster with an applied magnetic field (~2.4 kG), which consists of a cylindrical microplasma source and a conical micronozzle. The microplasma is sustained by microwaves and the propellant gas of Ar is heated up due to collisions between energetic electrons and neutrals. In order to decrease the diffusion loss of electrons due to the large surface-to-volume ratio in the microplasma chamber, we applied a strong axial magnetic field. The results of the thrust measurement have indicated that the thrust performance with the magnetic field are improved by 2.8 to 12.3% compared with the case without the magnetic field at the microwave power of 6 W and high mass flow rates (> 20 sccm).

Nomenclature

F_t	=	thrust
F_0	=	thrust in cold-gas operation
g	=	standard acceleration of gravity
I_{sp}	=	specific impulse
$\dot{m}$	=	mass flow rate
P	=	power
η	=	thrust efficiency

I. Introduction

IN recent years, the trend of space systems has been focused on miniaturization and simplification of the structure, to decrease the mission costs and to increase the launch rates. Missions with numerous small-scale satellites would bring a significant advantage of reducing the mission risk.[1] Such concept has supported a new approach to develop accurate, reliable, and low-cost micropropulsion systems, particularly for high-accuracy station keeping and attitude control.

In this paper, we report the performance of a microwave-excited microplasma thruster with an applied magnetic field. An advantage of microwave plasmas is that there is no electrode; thus, a serious lifetime problem caused by plasma sputtering is avoided. However, diffusion loss is a significant problem for the microplasma source due to the

[1] Graduate Student, Department of Aeronautics and Astronautics, Email: t.kawanabe@kw8.ecs.kyoto-u.ac.jp.
[2] Ph.D. Candidate, Department of Aeronautics and Astronautics, Email: rainbowmd81@gmail.com.
[3] Assistant Professor, Department of Aeronautics and Astronautics, Email: takao@kuaero.kyoto-u.ac.jp.
[4] Associate Professor, Department of Aeronautics and Astronautics, Email: eriguchi@kuaero.kyoto-u.ac.jp.
[5] Professor, Department of Aeronautics and Astronautics, Email:ono@kuaero.kyoto-u.ac.jp.

large surface-to-volume ratio. Applying a magnetic field is a way to reduce diffusion loss to the wall because electrons are strongly affected by the magnetic fields and confined along magnetic field lines, and ions are also confined by ambipolar effects even though ions are unmagnetized. We studied thrust performance of the microplasma thruster using 4-GHz microwaves with or without the magnetic field.

Microwaves propagate through a coaxial cable which is connected to the left end of the plasma chamber, where Ar gas used as the propellant in the present study is ionized and heated up by microwaves at pressures on the order of 10 kPa. Such high thermal energy is converted into directional kinetic energy through the nozzle, which has a converging and diverging section, to obtain the thrust.

II. Experimental Setup

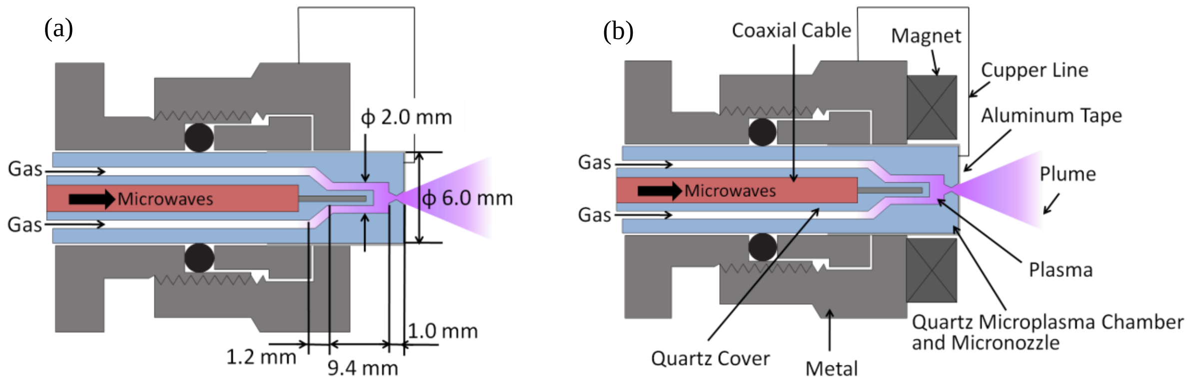

Figure 1. Cross-sectional views of a microplasma thruster (a) without a magnet and (b) with a magnet.

Figure 1(a) shows a cross-sectional view of the microplasma thruster without a magnet, which consists of an azimuthally symmetric microwave-excited plasma source and a conical micronozzle for exhausting the plasma.[2-7] Figure 1(b) shows a cross-sectional view of that with a magnet, and Fig. 2 shows a schematic view of the axial diverging field created by the magnet. The microplasma source is composed of a dielectric chamber made of quartz and a metal (Ultra-torr) around the chamber. The top of quartz cover is surrounded by aluminium tape and connected to the metal through a cupper line in order to avoid the leakage of microwaves and eliminate the electric potential between the metal and quartz. The inner and outer diameters of the dielectric chamber are 2.0 mm and 6.0 mm, respectively, and the length of the chamber is 10.6 mm for 4 GHz. The chamber length corresponds approximately to $\lambda/4$, where λ is the wave length of microwaves in dielectric (quartz).

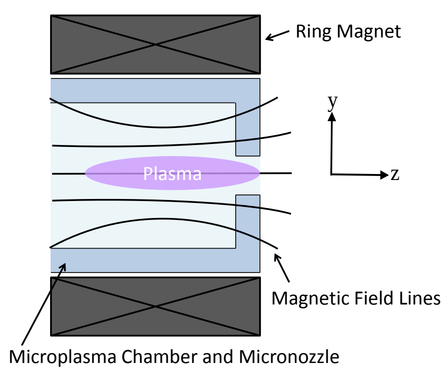

Figure 2. Schematic view of axial diverging field created by an axially magnetized ring magnet.

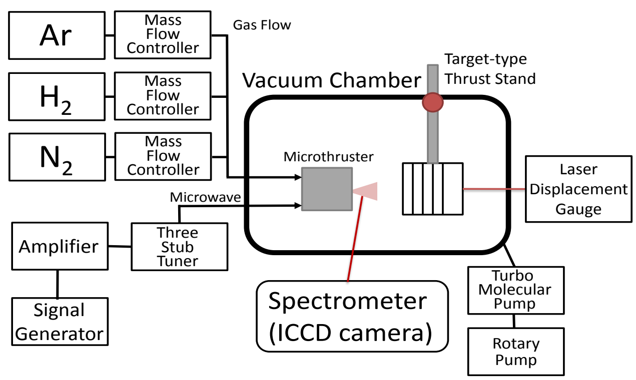

Figure 3. Experimental setup.

Figure 3 shows a schematic of the experimental setup. Microwaves (< 10 W) generated by a signal generator (Agilent E8257C) and an amplifier can propagate through a coaxial semi-rigid cable (RG-405/U) in the transverse electromagnetic (TEM) mode. The plasma is ignited using a tesla coil. Once the plasma is ignited, the discharge is sustained by microwaves. The reflection of microwave is nearly zero by adjusting a three stub tuner. The micronozzle has a diverging-converging section (Laval nozzle) which is fabricated by using conventional machining process with a diamond drill. The inlet, throat, and exit diameter of micronozzle are 0.6, 0.2, 0.8 mm, respectively, and the length of the micronozzle is 1.0 mm. The magnet is placed to enclose the top of the quartz chamber as shown in Fig. 1(b). The ring magnet is made of Ne–Fe–B, which has a residual magnetic field of about 11.4 kG, an outer diameter of 13.0 mm, an inner diameter of 7.0 mm, and a length of 10.0 mm. To measure the thrust performance, we use a target-type thrust stand for plasma-discharging operation and pendulum-type thrust stand for cold-gas operation.

A. Static Magnetic Field Analysis

A two-dimensional static magnetic field analysis was performed with ANSYS software. Figures 4(a) and (b) show the two-dimensional distributions of magnetic flux density and magnetic field lines generated by the ring magnet, respectively. In the microplasma chamber (radial position: $r < 2$ mm), magnetic field line is almost along the axial direction as shown in Fig. 4(b), which would impede energetic electron diffusion in radial direction.

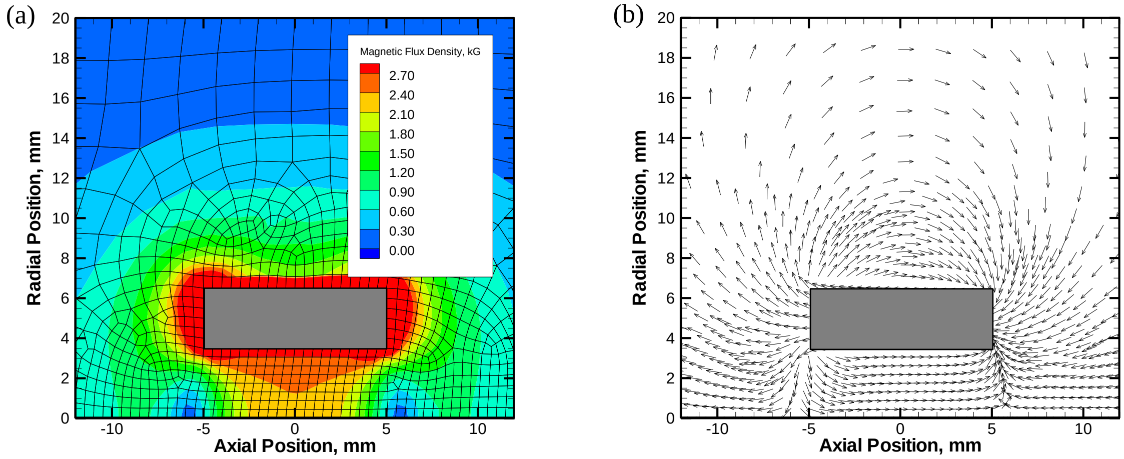

Figure 4. Two-dimensional distributions of the calculated (a)magnetic flux density and (b)magnetic field lines.

Figure 5(a) shows the calculated axial magnetic flux density as a function of axial position on the centerline ($r = 0$ mm) of the magnet. The peak axial magnetic flux density on the centerline is about 2.4 kG. Figure 5(b) shows the comparison between calculated and measured axial magnetic field values, which were measured with a gauss meter (F.W.Bell, 4048). The calculated value is in good agreement with the measured one as shown in Fig. 5(b). The measurement inside the inner ring magnet could not be conducted because there was no space to insert the probe, and thus we measured it only over the axial range of 6-10 mm.

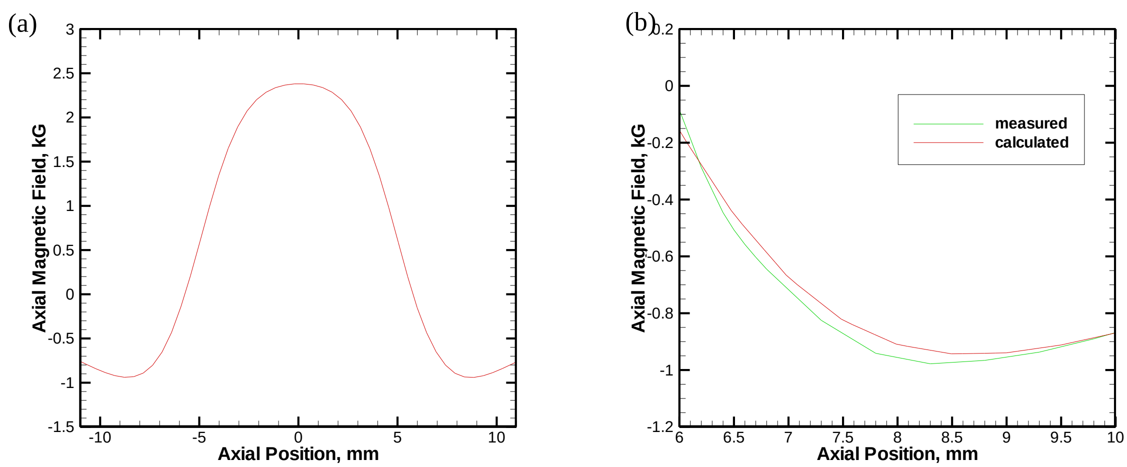

Figure 5. (a)Calculated axial magnetic field on the centerline and (b)comparison between calculated and measured values on the centerline.

B. Thrust Measurement

A pendulum method and target method are used for thrust measurement.[3] To measure the thrust performance, firstly the microthruster is mounted on the pendulum instead of the target as shown in Fig. 6, and then the displacement of the thruster in cold-gas operation is obtained as a function of mass flow rate. The microthruster and pendulum are installed in a stainless steel vacuum chamber evacuated by a rotary and turbo-molecular pump. The displacement of the pendulum is detected by a laser sensor (Keyence, LK-G85), where the resolution is about ±0.2 μm. The relation between the displacement and force is calibrated in advance by hanging some small weights of 13.6-23.5 mg with a thin wire 10 μm in diameter. Then, the thrust in cold-gas operation is determined as a function of mass flow rate. This procedure is referred to as the pendulum method.[8-10]

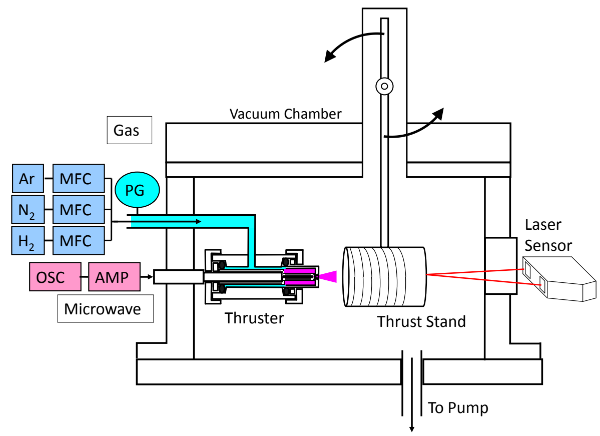

Figure 6. Schematic view of the experimental setup for the thrust measurement using the target thrust stand.

Secondly, the cylindrical target is mounted on the pendulum as shown in Fig. 6. The plasma plume ejected from the thruster hits a cylindrical target, mounted on one end of a pendulum with some weights being on the other end for balance. Figures 7(a) and 7(b) show the front and side views of the cylindrical target, similar to the one made by Yanagi and Kimura.[11] The plasma beam comes into the target made of Teflon, through the entrance hole on the front plate. The bottom plate of the target is conically shaped, and most rebounding gas particles from the bottom plate leave radially from the target through a number of slits on the side of the cylinder; in practice, the total opening area normal to the side is much larger compared with the area of the entrance hole. Thus, it is expected that the effect of rebounding particles on thrust measurement is negligible with this target.

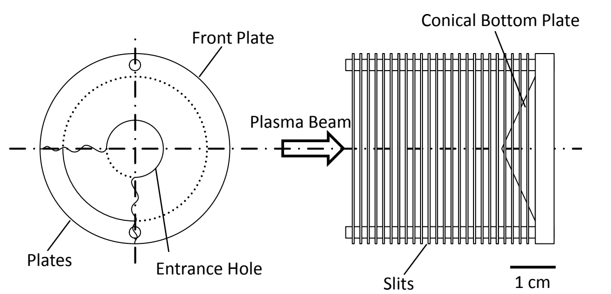

Figure 7. (a)Front and (b)side views of the cylindrical target made of Teflon.

In the same way as the pendulum method, the displacement of the target in plasma-discharging operation is obtained as a function of mass flow rate. The pendulum rotates around fulcrums of two knife edges without friction. The calibration is carried out by detecting the displacement of the target in cold-gas operation by changing the mass flow rate of 10-70 sccm and using the relationship between the mass flow rate and the thrust in cold-gas operation obtained by the pendulum method. To confirm the accuracy of the thrust measurement by the target method, we compare the thrust obtained by the pendulum method with that by the target method in cold-gas operation. After the difference between the thrust performances measured by the two methods is confirmed to be negligible, the thrust in plasma-discharging operation is obtained by the target method.

One might imagine that it is much easier and more accurate to measure the thrust by the pendulum method in plasma-discharging operation. However, microwaves are injected into the thruster through semirigid or flexible coaxial cables, which are much thicker and more rigid than those for dc and rf circuits. In addition, the microwave energy is easily converted into thermal energy during propagation through coaxial cables, and thus the thermal expansion of cables significantly degrades the signal-to-noise (S/N) ratio during the thrust measurement.

Once the thrust F_t is measured, the specific impulse I_{sp} is determined using the mass flow rate $\dot{m}$ and the standard acceleration of gravity g as

$$I_{sp} = F_t / \dot{m} g \tag{1}$$

In plasma-discharging operation, the thrust efficiency η is estimated from

$$\eta = F_t^2 / (2\,\dot{m} P + F_0^2) \tag{2}$$

where F_t is the thrust in plasma-discharging operation, F_0 is the thrust in cold-gas operation, and P is the microwave power absorbed in the thruster.

The thrust measurement was conducted at least five times for each experiment. The symbols in the figures shown below represent the average value, and the error is within 10%. Note that the error of the specific impulse have a tendency to become larger with decreasing mass flow rate, because the relative error of the mass flow rate resulting from the accuracy of the mass flow controller is larger at lower gas flow rates.

III. Results and Discussion

Figures 8 show the thrust as a function of mass flow rate in cold-gas and plasma-discharging operation with and without the magnet at the microwave power of 3 W (Fig. 8(a)) and 6 W (Fig. 8(b)). Note that the thrust in cold-gas operation is measured by pendulum method and the thrust in plasma-discharging operation is measured by target method.

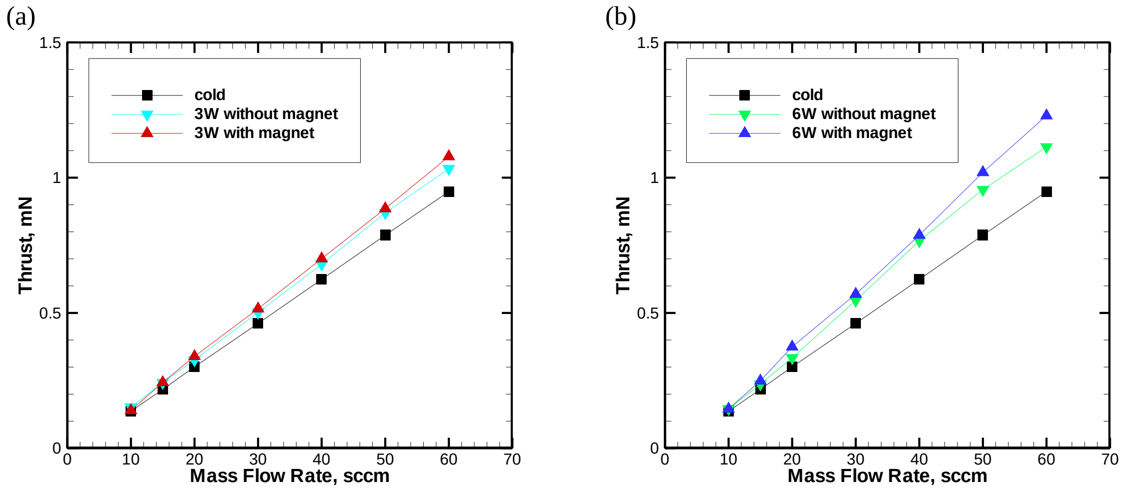

Figure 8. Thrust measured as a function of gas flow rate in cold-gas and plasma-discharging operation with and without the magnet at the microwave power of (a) 3 W and (b) 6 W.

Figure 9 shows the specific impulse in cold-gas and plasma-discharging operation with and without the magnet as a function of mass flow rate, calculated by substituting the thrust obtained the thrust measurement and the mass flow rate into Eq. (1). Figure 10 shows the thrust efficiency, which is also calculated by substituting the thrust both in plasma-discharging and cold-gas operation and input microwave power and the mass flow rate into Eq. (2) and plotted as a function of mass flow rate.

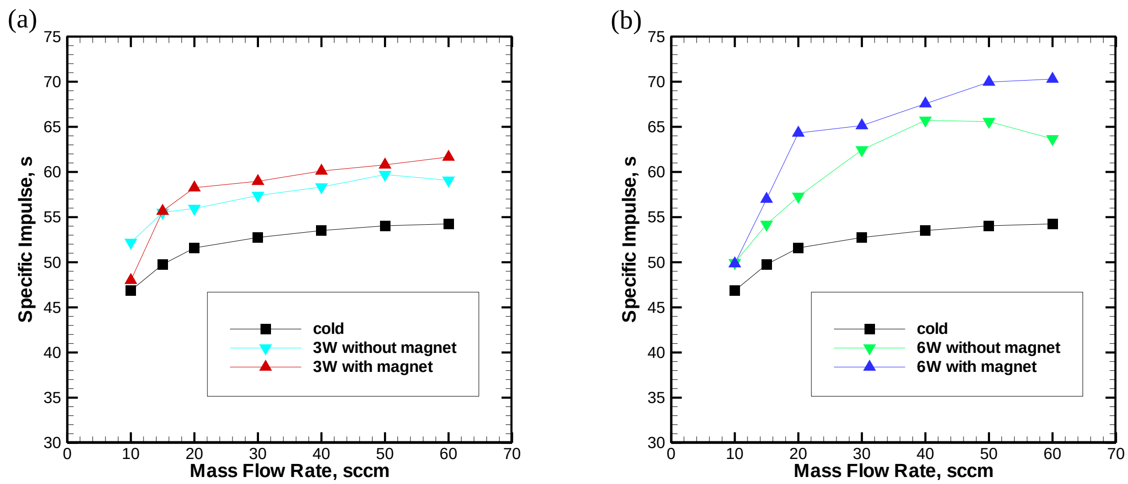

Figure 9. Specific impulse as a function of gas flow rate in cold-gas and plasma-discharging operation with and without the magnet at the microwave power of (a) 3 W and (b) 6 W.

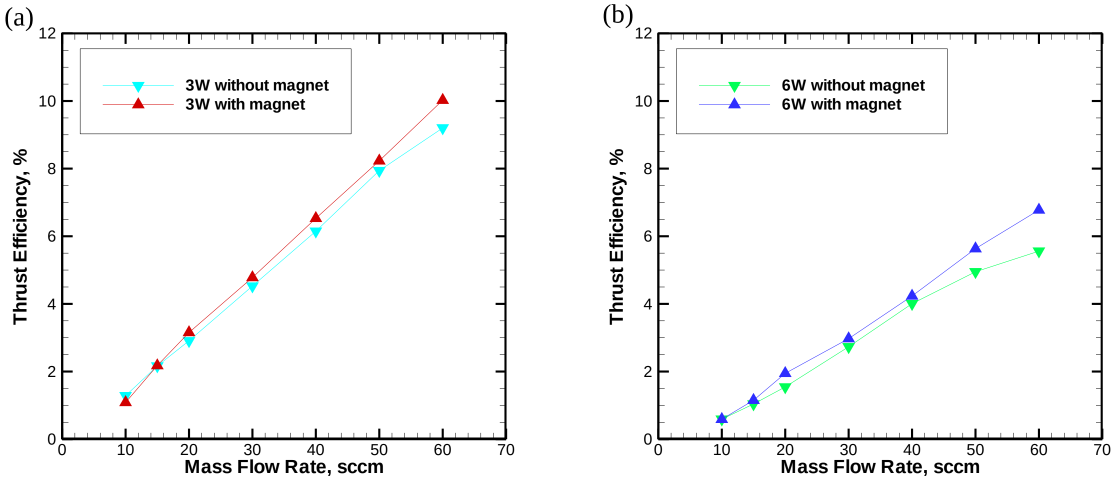

Figure 10. Thrust efficiency as a function of gas flow rate in cold-gas and plasma-discharging operation with and without the magnet at the microwave power of (a) 3 W and (b) 6 W.

Although the difference of the thrust between plasma-discharging operation with and without a magnet is basically within the error, the results focused on the average value indicate that the thrust obtained in plasma-discharging operation with the magnet is several percent higher than that without the magnet at high gas flow rates (> 20 sccm). Under this condition, the thrust obtained with the magnet is increased by 1.8-5.6% compared with that without the magnet at the microwave power of 3 W. Similarly, the thrust is increased by 2.8-12.3% at the microwave power of 6 W.

In the case of microwave power of 3 W at the gas flow rate of 60 sccm, the thrust obtained is 1.08 mN with the magnet, giving the specific impulse of 62 s and thrust efficiency of 10.0%, whereas the thrust obtained is 1.03 mN without the magnet, giving the specific impulse of 59 s and thrust efficiency of 9.2%. In the case of microwave power of 6 W at the gas flow rate of 60 sccm, the thrust obtained is 1.23 mN at the microwave power of 6 W with the magnet, giving the specific impulse of 70 s and thrust efficiency of 6.8%, whereas the thrust obtained is 1.11 mN at the microwave power of 6 W without the magnet, giving the specific impulse of 64 s and thrust efficiency of 5.6%.

The difference of the thrust performance between with and without the magnet seems to depend on the microwave power as shown in Figs. 8-10, which indicates that the effect of applying magnetic field would occur clearly at higher microwave powers. This is probably because more energetic electrons are generated by increasing microwave power, and then, they are interacted with the strong magnetic field in the microplasma chamber. Thus, more electrons would collide with heavy particles more often prior to the direct loss to the wall. Moreover, heavy particle temperature would be increased; finally, the thrust would be increased. At lower mass flow rates, rarefaction effect would be dominant; therefore, the specific impulse becomes lower than at higher mass flow rates as shown in Fig. 9. The difference of the thrust between plasma-discharging operation with and without the magnet is so small at low mass flow rate, and it is possible that plasma-discharging operation with the magnet does not effectively improve the thrust performance compared with that without the magnet. If the thrust performance in the case with the magnet is worse than that without the magnet at low mass flow rates, some loss mechanisms caused by applying magnetic field would exist, such as increasing inelastic collisions between electrons and heavy particles, and increasing the direct loss of electrons to the wall running along axial magnetic field lines even though they are well confined in radial direction. It is necessary to further investigate the magnetic field shape and strength to confine energetic electrons sufficiently.

IV. Conclusion

A thrust measurement of microwave-excited microplasma thruster with and without an applied axial magnetic field were performed in order to investigate the effectiveness of applying magnetic fields. The results indicate that the thrust obtained in plasma-discharging operation with the magnet increases by 2.8 to 12.3% compared with that without the magnet at high gas flow rates and the microwave power of 6 W. However, at low mass flow rates, we could not obtain a clear improvement of the thrust performance with the magnet. Optical emission spectroscopy measurement is underway in order to investigate the electron density and gas temperature and the result will be presented at the conference.

References

[1] Mueller, J., "Thruster Options for Microspacecraft: A Review and Evaluation of Existing Hardware and Emerging Technologies," *Proceedings of the 33rd AIAA/ASME/SAE/ASEE Joint Propulsion Conference,* Paper No. AIAA Paper 97-3058, AIAA, Seattle, WA, 1997.

[2] Takao, Y. and Ono, K., "A miniature electrothermal thruster using microwave-excited plasmas: a numerical design consideration," *Plasma Sources Science and Technology,* Vol. 15, No.2, May. 2006, pp. 211-227.

[3] Takao, Y., Eriguchi, K., and Ono, K., "A miniature electrothermal thruster using microwave-excited microplasmas: Thrust measurement and its comparison with numerical analysis," *Journal of Applied Physics,* Vol.101, No. 12, 15 Jun. 2007, pp. 123307-1-10.

[4] Takahashi, T., Takao, Y., Eriguchi, K., and Ono, K., "Microwave-excited microplasma thruster: a numerical and experimental study of the plasma generation and micronozzle flow," *Journal of Physics D: Applied Physics,* Vol. 41, No. 19, 7 Oct. 2008, pp. 194005-1-6.

[5] Takao, Y., Takahashi, T., Eriguchi, K., and Ono, K., "Microplasma thruster for ultra-small satellites: Plasma chemical and aerodynamical aspects," *Pure and Applied Chemistry,* Vol. 80, No. 9, 26-31 Aug. 2007, pp. 2013-2023.

[6] Takahashi, T., Takao, Y., Eriguchi, K., and Ono, K., "Numerical and experimental study of microwave-excited microplasma and micronozzle flow for a microplasma thruster," *Physics of Plasmas,* Vol. 16, No. 8, Aug. 2009, pp. 083505-1-14.

[7] Takahashi, T., "Numerical and Experimental Study of Performance Improvement of a Microwave-Excited Microplasma thruster Designed for Small Spacecraft," Ph.D. Dissertation, Aeronautics and Astronautics Dept., Kyoto Univ., Kyoto, JP, 2011 (to be published).

[8] Orieux, S., Rossi, C., and Estève, D., "Thrust stand for ground tests of solid propellant microthrusters," *Review of Scientific Instruments,* Vol. 73, No. 7, Jul. 2002, pp. 2694-2698.

[9] Takahashi, K., Lafleur, T., Charles, C., Alexander, P., Boswell, R.W., Perren, M., Laine, R., Pottinger, S., Lappas, V., Harle, T., and Lamprou, D., "Direct thrust measurement of a permanent magnet helicon double layer thruster," *Applied Physics Letters,* Vol. 98, No. 14, 4 Apr. 2011, pp. 141503-1-3.

[10] Sasoh, A., Arakawa, Y., "A high-resolution thrust stand for ground tests of low-thrust space propulsion devices," *Review of Scientific Instruments,* Vol. 64, No.3, Mar. 1993, pp. 719-723.

[11] Yanagi, R., Kimura, I., "New Type of Target for the Measurement of Impulse Bits of Pulsed Plasma Thrusters," *Journal of spacecraft and rockets,* Vol. 19, No.3, 1982, pp. 246-249.